from files
JUN 11 1965
A/CONF.28/P/12

PAPERS PRESENTED BY CANADA TO THE THIRD U.N. INTERNATIONAL CONFERENCE
ON THE PEACEFUL USES OF ATOMIC ENERGY, GENEVA, 31 AUG — 9 SEP, 1964

Research with Inelastic Neutron Scattering at the NRU Reactor

by

B.N. Brockhouse
McMaster University, Hamilton, Ontario

A.D.B. Woods, G. Dolling and I.M. Thorson
Chalk River Nuclear Laboratories,
Atomic Energy of Canada Limited,
Chalk River, Ontario

AECL-2012

DISCLAIMER

Portions of this document may be illegible in electronic image products. Images are produced from the best available original document.

RESEARCH WITH INELASTIC NEUTRON SCATTERING AT THE NRU REACTOR

B.N. Brockhouse,
McMaster University, Hamilton, Ontario

A.D.B. Woods, G. Dolling and I.M. Thorson,
Chalk River Nuclear Laboratories,
Atomic Energy of Canada Limited, Chalk River, Ontario

1. INTRODUCTION

Beams from high-flux reactors provide neutrons in quantities large enough to permit the convenient exploration of the structure of solids and liquids. The neutrons are probes with which the experimenter can determine the relative positions of the atomic nuclei and their movements in space and time.

Given a nucleus at position r = 0 and time t = 0, the probability that there will be a nucleus at position $\vec{r}$ and time t is expressed by the Van Hove space-time correlation function $G(\vec{r}, t)$ [1]. Information about $G(\vec{r}, t)$ may be obtained from measurements of the cross-section for the scattering of slow neutrons by the system of nuclei, because of the double Fourier transform relationship

$$S(\vec{Q}, \omega) = \frac{1}{2\pi} \iint \exp i(\vec{Q}.\vec{r} - \omega t)\, G(\vec{r}, t) d\vec{r}\, dt \qquad 1$$

The function $S(\vec{Q}, \omega)$ is directly related to the partial differential scattering cross-section. If the incident and scattered neutrons have energies E_o and E', and wave vectors $\vec{k_o}$ and $\vec{k'}$, then their momentum-transfer vector $\vec{Q}$ and energy transfer ϵ are given by $\vec{Q} = \vec{k_o} - \vec{k'}$ and $\epsilon = \hbar\omega = E_o - E'$ respectively. It is convenient to divide the cross-section into a <u>coherent</u> part and an <u>incoherent</u> part; the former contains effects of interference between the scattering from pairs of atoms, the latter is related to the behaviour of a single atom.

In a crystalline solid, the nuclei vibrate about a set of equilibrium positions making up a regular three-dimensional array. Under the approximation that the interatomic forces are harmonic, the nuclear motions may be represented by a family of non-interacting plane waves, each associated with a wave vector $\vec{q}$ (q is 2π times the reciprocal of the wavelength) a frequency ν, and a polarization index j. The coherent part of the scattering cross-section can then be decomposed into terms involving the creation or

annihilation of 0, 1, 2 ... quanta (phonons) of these waves. The "one-phonon" term is of primary importance for the study of the frequency/wave-vector dispersion relation $\nu = \nu_j(\vec{q})$ for a solid, owing to the presence of two δ-functions expressing conservation of "crystal momentum" and conservation of energy:

$$\vec{Q} = \vec{k_o} - \vec{k'} = 2\pi\vec{\tau} + \vec{q} \qquad 2$$

$$\hbar\omega = E_o - E' = h\nu \qquad 3$$

where $\vec{\tau}$ is a vector of the reciprocal lattice of the crystal. Thus the energy distribution of initially monoenergetic neutrons, after coherent one-phonon scattering at a particular angle from a single-crystal specimen, consists (ideally) of a small number of δ-function peaks. From the location of each peak, the frequency and wave vector of the phonon concerned may be deduced by means of eqs. 2 and 3. The incoherent part of the scattering does not contain the δ-function expressed by eq. 2 and is therefore less informative. It is sometimes possible, however, to derive the frequency-distribution function $g(\nu)$ from measurements of incoherent one-phonon scattering.

The dynamics of a coupled system of magnetic moments can similarly be described in terms of correlation functions and dispersion relations, which are accessible to experimental determination by neutron inelastic scattering.

2. TECHNIQUES

Four spectrometers designed to measure $S(\vec{Q}, \omega)$ and the $\vec{Q}$ and $\hbar\omega$ of the "one-phonon" groups have been in use at the NRU reactor in Chalk River for several years. These instruments fall into two classes: (a) those which utilize Bragg reflection of neutrons from large single crystals both to select a monoenergetic neutron beam from the Maxwellian reactor spectrum and to measure the wavelength of the scattered neutrons and (b) those which utilize a chopper system to produce pulsed monoenergetic incident neutron beams and time-of-flight measurements over a known distance to determine the neutron velocity after scattering from the specimen.

Often the design requirements for spectrometers used for $\nu(\vec{q})$ measurements in crystals and for $S(\vec{Q}, \omega)$ measurements for use in reactor-spectra calculations are different. In particular, for determinations of $\nu(\vec{q})$ it is desirable to measure, under conditions of high resolution, the energy distributions of those neutrons scattered at a preselected value of $\vec{Q}$; for this purpose a crystal spectrometer is convenient. For measurements of $S(\vec{Q}, \omega)$ it is desirable to make observations of the scattered neutrons over a large range of energy and momentum transfers, and here pulsed-beam spectrometers have an advantage since a large number of counters at various scattering angles can be used simultaneously.

2.1 Crystal Spectrometers

2.1.1 The triple-axis spectrometer [2,3]. This is shown schematically in Fig. 1. Neutrons from the reactor impinge on the monochromator crystal X1 in the centre of the large shielding drum. Monoenergetic neutrons are selected from the beam by Bragg reflection through the angle of scattering $2\theta_m$. This angle is continuously variable and the crystal X1 automatically follows at half the angular speed. In addition various planes in the crystal X1 can be selected. Thus thermal neutrons of any desired wavelength can be selected.

The orientation of the specimen, S, about its vertical axis is defined by the angle ψ and the angle of scattering at S by the angle ϕ. Both these angles are continuously variable. The energies of the neutrons scattered from S are determined by Bragg reflection from the analysing crystal X2, though the angle $2\theta_a$, into the $^{10}BF_3$ counter.

It is desirable in measurements of $\nu(\vec{q})$ in crystals to observe neutron-energy distributions while holding $\vec{Q}$, and hence $\vec{q}$, constant. This can be done by moving three of the four angles, $2\theta_m$, ψ, ϕ, $2\theta_a$, simultaneously in a predetermined manner. In the usual practice $2\theta_a$ is held constant, and $2\theta_m$ is treated as the independent variable. A computer program gives the (non-linear) variation of ψ and ϕ required to maintain the preselected value of $\vec{Q}$. The computer output, punched on paper tape, is fed into the spectrometer; the indicated angular movements are carried out electrically. In this way neutron-energy distributions can be observed automatically at any desired number of successive values of $\vec{Q}$. In this method any observed neutron group occurs at a useful value of $\vec{q}$; thus conduct of the experiments and handling of data are both done very efficiently. In addition to the constant-$\vec{Q}$ technique, other variations, valuable for particular experiments, are possible [2].

2.1.2 Beryllium-detector spectrometer. Certain types of measurement, particularly of incoherent scattering involving large energy transfers (e.g. in the study of vibrations in hydrogenous compounds) can be very efficiently made by means of the beryllium-detector technique. In the Chalk River version, the triple-axis spectrometer (Fig. 1) is modified by removing the analyser crystal X2 and placing 10 cm of polycrystalline beryllium in front of the $^{10}BF_3$ counter; then only those scattered neutrons with energies less than the beryllium cut-off (5 meV) can be detected. The scattered-neutron intensity is observed as a function of the (variable) energy of the incident beam.

2.1.3 Spectrometer for investigations of liquid helium. A specialized crystal spectrometer which has been used principally for investigations of liquid helium was designed by D.G. Henshaw. A beam of cross-section 25 cm x 25 cm from the reactor is passed through 25 cm of beryllium cooled by liquid nitrogen and other filter material. The filter transmits only those neutrons with wavelengths longer than 3.95 Å. From this beam neutrons of wavelength 4.04 Å are selected by Bragg reflection from the (111) plane of aluminum single crystal. The angle of scattering of neutrons from the specimen of

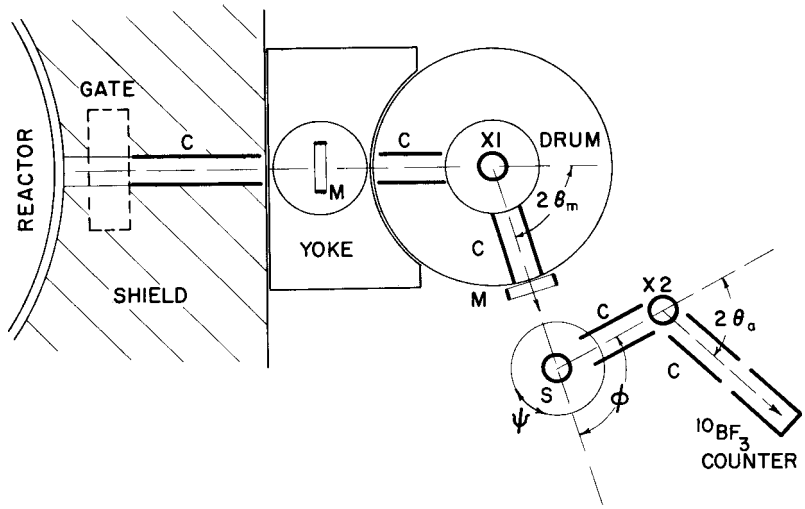

Fig. 1 - The triple-axis crystal spectrometer (schematic). C = collimator M = fission-chamber monitor.

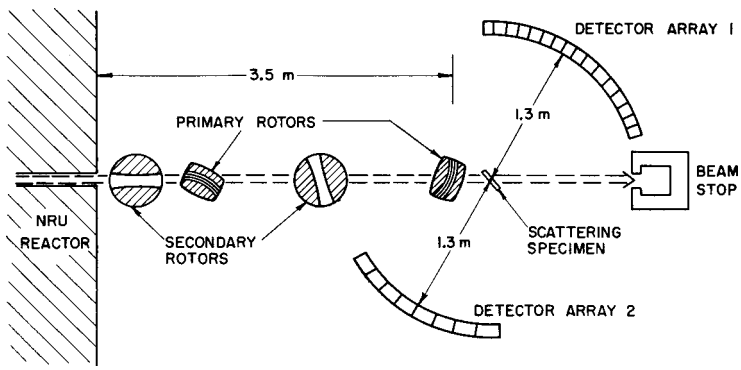

Fig. 2 - The phased-rotor spectrometer (schematic). The primary rotors spin at twice the frequency of the secondary rotors. Fission-chamber monitor detectors in the incident beam (not shown) are used to determine the incident-neutron velocity and the time of arrival of each neutron pulse at the scattering specimen.

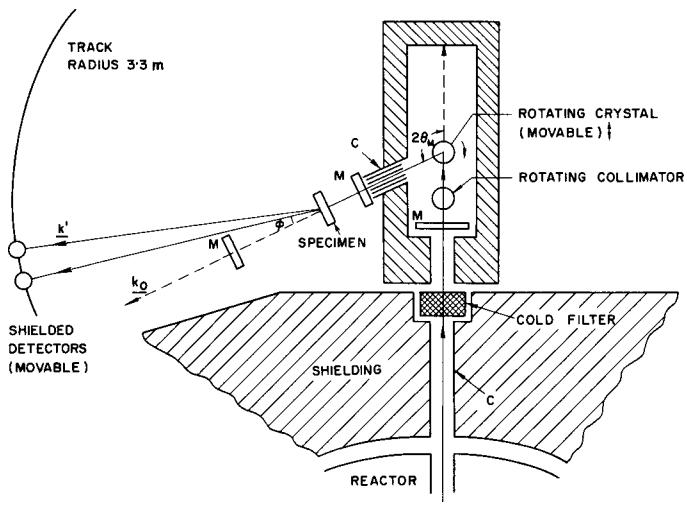

Fig. 3 - The rotating-crystal spectrometer (schematic). C = collimator M = fission-chamber monitor.

liquid helium can be varied from 0° to 140°. The energies of the scattered neutrons are then determined by Bragg reflection from a lead analysing crystal. The energy resolution of this spectrometer (E_o = 5 meV) is about 0.2 meV.

2.2 Pulsed-Beam Spectrometers

2.2.1 Phased-rotor spectrometer. The primary rotors of the spectrometer [5] shown in Fig. 2 are 20 cm in diameter and spin synchronously at 500 Hz. Only those neutrons which traverse the 2.74-m flight path between the primary rotors during the interval defined by their relative phasing are transmitted. Twelve curved slots in the primary rotors transmit a beam 2.5 cm high by 5.0 cm wide of up to 10^4 n/s in bursts whose standard deviation in time of arrival at the scattering specimen and reciprocal velocity are 2.3 μs and 0.9 μs/m respectively. The secondary rotors scatter those fast neutrons which leak through the primary rotors. All four rotors are driven by hysteresis motors powered by a common oscillator-amplifier system.

Neutrons scattered by the specimen are detected in 20 to 25 LiF-ZnS scintillators concurrently. The energy distributions of the scattered neutrons are determined from their times of flight from the specimen to the detectors. One of three detector assemblies may be used, with detectors ranging in size from 5.0 cm diameter to 7.5 cm by 15 cm. For maximum angular coverage, detectors are operated from 10° to 160° at 1.3 m from the specimen. For higher-resolution experiments, detectors may be operated at small angles, 4° to 26°, or at 50° to 120°, both arrays being at a distance of 3.0 m from the specimen. Each detected event is encoded as to detector and time channel of origin and recorded on a magnetic tape. The tape is subsequently scanned and the information is sorted and punched on cards ready for processing on a computer. Cross-sections are determined by comparing the counting rates in the detectors with that in a fission-chamber monitor in the main beam.

2.2.2 Rotating-crystal spectrometer. A schematic diagram of the rotating-crystal spectrometer [2] is shown in Fig. 3. Pulses of monoenergetic neutrons, with wavelengths determined by the Bragg law, are produced whenever the rotating crystal comes into a reflecting position. This pulsed beam is scattered by the specimen, and the energies of the scattered neutrons are determined by electronic measurement of their times of flight over the distance (3.3 m) from the specimen to the counters. Events are now recorded on magnetic tape and sorted via a direct line to a computer. A Soller-slit collimator rotating in phase with the monochromator, eliminates order contamination in the incident beam. At 5 meV the resolution of this instrument is about 0.2 meV.

3. CRYSTAL DYNAMICS

The phenomenological theory of the thermal vibrations of the atoms in a crystalline solid is presented in detail by Born and Huang [6]. In the theory, the frequencies of the normal modes of vibration are given by the

eigenvalues of a 3n x 3n "dynamical matrix" (n is the number of atoms in the primitive unit cell) whose elements are function of the force constants that represent the (harmonic) forces between pairs of atoms in the crystal. In the harmonic approximation, neutrons, scattered with creation or annihilation of one phonon, occur as groups (in the energy and momentum distributions) which are represented mathematically by δ-functions with the arguments of eqs. 2 and 3. The groups, broadened only by instrumental resolution, correspond to phonon frequencies which are independent of temperature. If, as for real solids, the interatomic forces are not purely harmonic, these δ-functions broaden into approximately Lorentzian peaks, and the phonon frequencies become temperature-dependent. Thus, observation of the energy width and shift of the neutron groups as a function of temperature can give information concerning the anharmonicity of interatomic forces in a solid.

As discussed in section 2, the triple-axis spectrometer enjoys distinct advantages over other machines in the application of this powerful method for investigating interatomic forces in crystals. Thus most of the work described below has been performed on the triple-axis instrument, though occasional use has been made of the rotating-crystal spectrometer.

Measurements of $\nu_j(\vec{q})$ have been made at 100°K on single crystals of sodium iodide [7], and at 296°K for niobium [8], molybdenum [9], tantalum [10], tungsten [11], nickel [12], pyrolytic graphite [13] and silicon [14, 15] (Pyrolytic graphite does not have the ideal structure of a true single crystal, and so only a very limited study of its dispersion relation has been possible). As an example of the kind of results which have been obtained, Fig. 4 shows the dispersion relation in three directions, Δ, Σ and Λ, in a single crystal of pure silicon [15]. Silicon has the diamond structure (two atoms per unit cell) and thus $\nu_j(\vec{q})$ consists of six "branches". In the Δ and Λ directions, only four branches are distinct because of the degeneracy of pairs of transverse modes. (Two of the six distinct branches in the Σ direction have not yet been studied.) These results have been analysed in terms of the dipole approximation model (developed by Cochran), two versions of which are represented by the solid and dashed curves shown in the figure. Although this model is probably over-simplified (its application to alkali halides has been more successful), the results strongly indicate the existence of long-range forces of electrostatic origin, which arise from the polarizability of the silicon atoms. Similar conclusions have been reached for germanium and gallium arsenide. Indeed, certain types of long-range forces, as revealed by analysis of $\nu_j(\vec{q})$ according to the Born-von Kármán theory, appear in most of the substances studied.

The thermal vibrations of lead [16, 17], sodium [18], β-brass (CuZn) [20], germanium [21], gallium arsenide [22], potassium bromide [7] and strontium titanate [23], have been studied also as functions of temperature. The experiments on lead provided valuable information concerning its Fermi surface; the experiments on strontium titanate have an important bearing on

the theory of ferroelectricity proposed by Cochran [24]. Fig. 5 illustrates the variation with temperature of a neutron group corresponding to a transverse mode of vibration in sodium; the increase in width and phonon-frequency shift are clearly observable. Fig. 6 shows neutron groups corresponding to the longitudinal and transverse optic modes of very long wavelength (but non-zero frequency) in potassium bromide. The relation, deduced by Lyddane, Sachs and Teller [25], between the ratio of these two frequencies and the static and high-frequency dielectric constants, was found to be obeyed in this case, and also for sodium iodide and gallium arsenide.

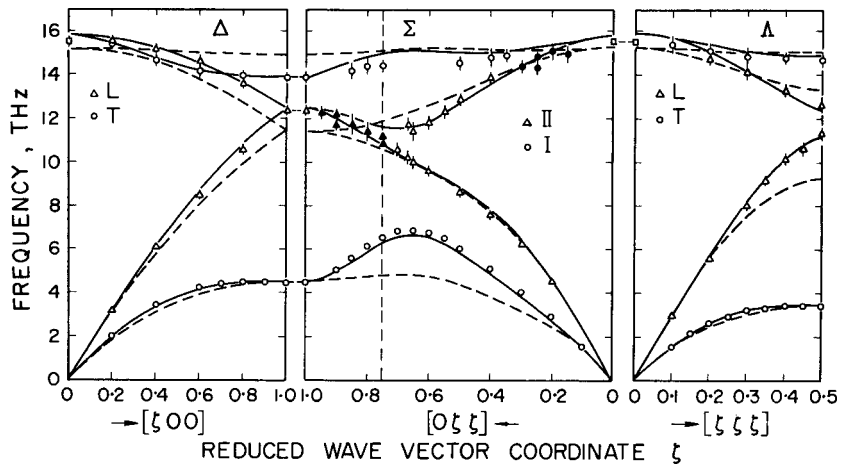

Fig. 4 - Experimental and theoretical dispersion curves for silicon at 296°K.
△ Longitudinal and type II [0ζζ] phonons.
○ Transverse and type I [0ζζ] phonons.
▲ ● Polarization undetermined.

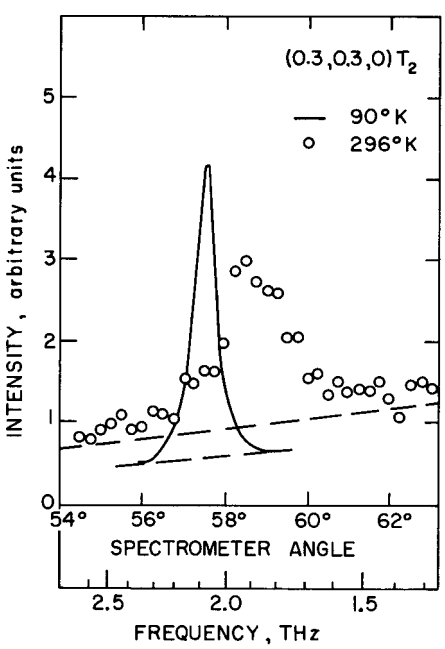

Fig. 5 - Temperature dependence of a neutron group associated with a particular mode of vibration in sodium.

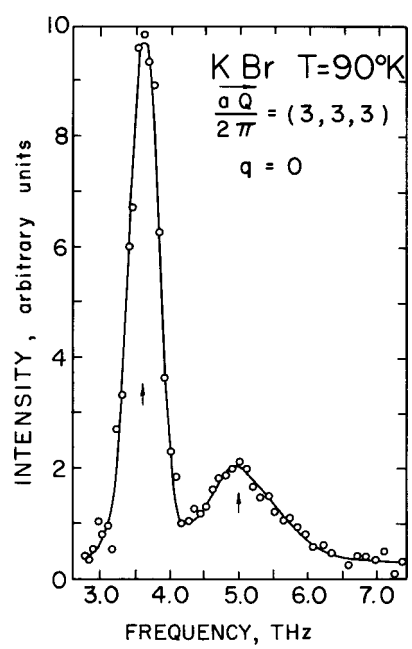

Fig. 6 - Neutron groups associated with transverse and longitudinal optic modes of vibration in potassium bromide.

4. LIQUID DYNAMICS

4.1 Liquid Helium

The thermodynamic and transport properties of liquid helium II can be explained on the assumption that the system is weakly excited above its ground state, and that there is a well defined relation (dispersion curve) between the energies, E, and momenta, p, of these excitations [26]. It was pointed out by Cohen and Feynman [27] that this dispersion curve could be determined by inelastic neutron scattering and such experiments have been carried out at several laboratories. The results, obtained [28] using the spectrometer described in section 2.1.3, are shown in Fig. 7 for liquid helium under its normal vapour pressure and also at a pressure of 25.3 atm. More recent experiments [29] using the rotating-crystal spectrometer indicate that the bending over of the curve at large values of momentum transfer ($p > 2.5$ Å^{-1}) continues such that in the limit $E \approx 2\Delta$, where Δ (8.65°K) is the energy at the minimum of the dispersion curve ($p = 1.91$ Å^{-1}). The intensities of the neutron groups are very low in this region. This behaviour is in accord with predictions of L.P. Pitaevskii [30].

4.2 Classical Liquids

The Van Hove correlation functions (see section 1) have been determined for several liquids. For liquid lead, a coherent scatterer, the complete pair correlation function G(r,t) was determined [31] for times from 0 to 2 ps, using the triple-axis spectrometer. For water (from which 95% of the scattering is incoherent scattering by the protons) the self-correlation function G(r,t) of the protons was determined [32, 33] for times from ~0.2 to 10 ps, by experiments using the rotating-crystal spectrometer. (For liquid lead all natural frequencies are much smaller than the melting temperature ($\hbar\omega \ll k_B T_M$); thus the classical correlation function has meaning, and may be determined, over the entire time range. For water, on the other hand, the correlation function has its classical interpretation only for comparatively long times, greater than $\hbar/k_B T_M$. In each case the long time limit was set by the experimental energy resolution.)

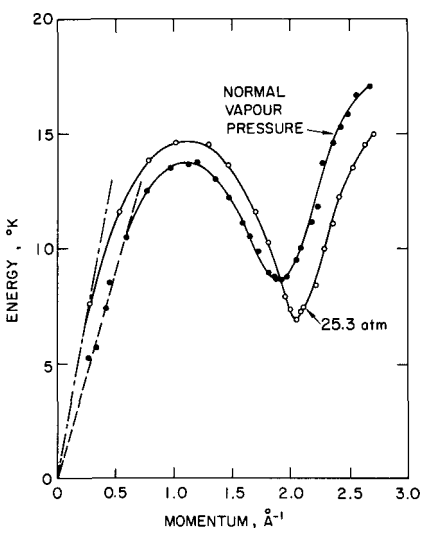

Fig. 7 - The dispersion relation for excitations in liquid helium II at two different pressures.

More recently correlation functions were determined for liquid argon over times up to 20 ps, by Dasannacharya and Rao [34]. In these experiments, measurements made by the rotating-crystal and the triple-axis spectrometers were combined. The results for the self-correlation function for liquid argon close to its triple point are shown in Fig. 8.

The main interest of the results lie in the light they cast on the diffusion mechanisms [35] in the liquid. For water and lead the results

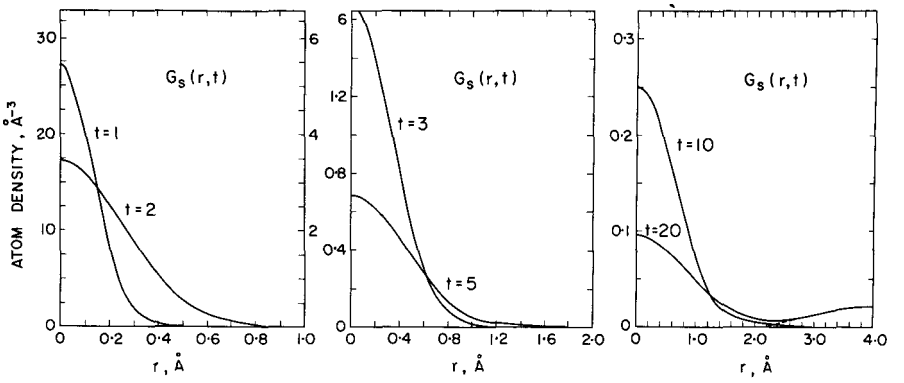

Fig. 8 - The self-correlation function $G_s(r,t)$ for argon near its triple point.

suggest that at small times and distances the mechanisms are complicated; for argon the results can apparently be described by simple diffusion theory.

5. MAGNETIC DYNAMICS

Magnetic inelastic scattering can be employed to study the dynamics of systems of coupled magnetic moments, in ways analogous to the study of crystal (and liquid) dynamics by means of nuclear inelastic scattering. The dynamics of any system of ordered magnetic moments can be described in terms of spin waves, the dispersion relation for which can be determined in the same way as the dispersion relation for lattice vibrations, by use of the conservation equations 2 and 3. The scattered neutrons fall into groups in the energy distribution corresponding to creation or annihilation of a single quantum ("magnon") of spin-wave energy. Neutron groups arising from interaction with magnons can be identified unambiguously from the response of their intensities to an applied magnetic field. Two materials have been studied so far, principally on the triple-axis spectrometer. (a) The lower part of the dispersion curve for the spin waves in a face-centred cubic alloy of cobalt with 8% iron was measured [36], and found to be substantially isotropic and parabolic in energy, as expected theoretically. (b) The acoustical branch and part of one optical branch of the dispersion curves were studied [37] for the ferrimagnetic substance, magnetite (Fe_3O_4). The results [38] are shown in Fig. 9 and are in substantial agreement with calculations by T.A. Kaplan [39] and by Glasser and Milford [40] based on the Néel model for the magnetic structure in ferrites.

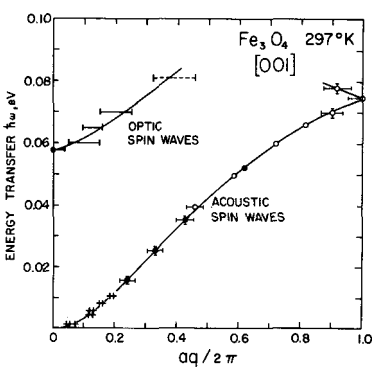

Fig 9 - Dispersion curves for spin waves in magnetite at 297°K.

The magnetic dynamics of paramagnetic substances can also be studied by neutron spectroscopy; in particular magnetic correlation functions can be determined. Where the largest interaction involved is that of the magnetic moment with the crystalline

electrostatic field, an energy spectrum which is substantially independent of wave vector is obtained. Fig. 10 shows results for erbium oxide; the lines observed represent transitions between various components of the ground-state multiplet of the free Er^{3+} ion, split in the crystalline field. The dependence of the width on temperature is probably the result of spin-lattice interaction.

6. CROSS-SECTIONS FOR SPECTRA CALCULATIONS

The scattering cross-sections for materials used in the construction of thermal reactors are of intrinsic interest for neutron-spectrum calculations, even though their interpretation in terms of the atomic motions may not yet be possible. Such spectra are seldom sensitive to the details of the cross-sections, but the range of energy and momentum transfer over which data are required is rather extensive. Several reactor materials have been studied in the energy region 0-0.1 eV, and momentum region 0.2-16 $Å^{-1}$, using the phased-rotor spectrometer. Some measurements on water taken at high energy resolution with the rotating-crystal spectrometer supplement these.

Light and heavy water at 298°K and 423°K have been studied [42, 43] and preliminary results have been taken at 553°K. Graphite has been studied [44, 45] at several temperatures, and UO_2 at 298°K and 783°K. Other materials such as Be and BeO [46] and ZrH [47] have also been studied at room temperature only.

In these experiments reciprocal velocity (i.e. wavelength) distributions of the scattered neutrons at 25 scattering angles from 10° to 160° are measured simultaneously on the phased-rotor spectrometer. An example of such a distribution is shown in Fig. 11 after corrections for background and detector efficiency have been made. The absolute cross-section scale is derived from measurements with a vanadium specimen and where possible the scale is checked by integration of the distributions over angle and energy and comparison with total cross-section values.

The wavelength distributions are transformed to give cross-section per unit-energy interval and solid angle $\partial^2\sigma/\partial\Omega\partial\epsilon$. These cross-sections are then reduced to a scattering function $S'(Q,\epsilon)$ by the relation -

$$\frac{\partial^2\sigma}{\partial\Omega\partial\epsilon} = \frac{k'}{k_o}\left\{e^{-\epsilon/2k_BT}\right\}\frac{\sigma_b}{4\pi}\, S'(Q,\epsilon) \qquad 4$$

where k' and k_o are as defined above (section 1), T is the specimen temperature and σ_b is the bound-atom cross-section of the constituent atoms. In the case of polyatomic materials eq. 4 must be generalized or σ_b chosen arbitrarily with consequent loss of physical significance for S'. The advantage of this formulation is that $S'(Q,\epsilon)$ is now an even function of ϵ and independent of the incident-neutron energy thus allowing a direct comparison

of experimental data taken under different experimental conditions.

Most of the scattering by H_2O comes from the protons and no significant errors are made by using the hydrogen scattering cross-section in eq. 4. Since the coherent scattering by protons is very small the scattering pattern from H_2O is sensitive only to the motions of the individual protons. The $S'(Q,\epsilon)$ function for protons in H_2O is given in Fig. 12. The results in the region of 0.05-0.08 eV appear to show less energy dependence that has been indicated from other studies but this apparent discrepancy arises from a combination of factors: the variation of S' with Q, the Boltzmann factor,

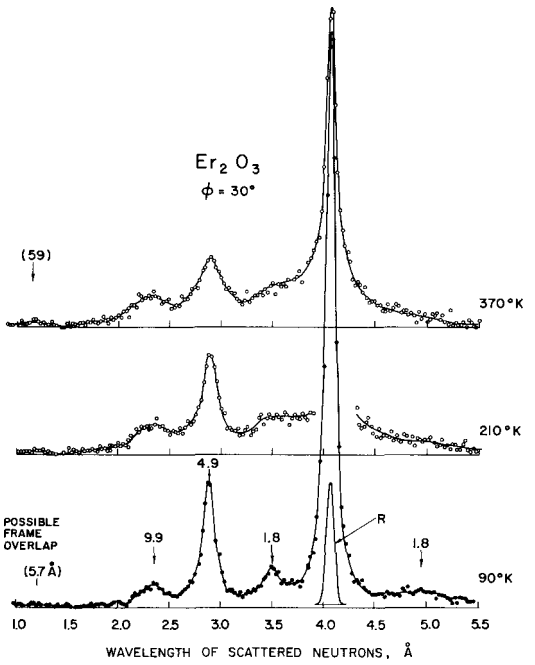

Fig. 10 - Wavelength distributions of neutrons scattered from erbium oxide at three temperatures.

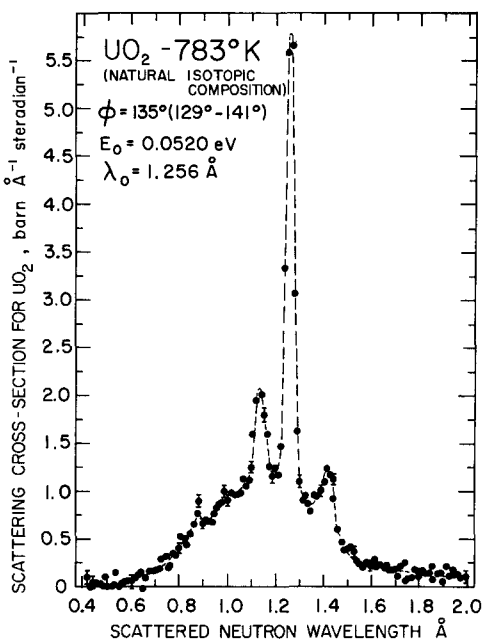

Fig. 11 - A wavelength distribution of neutrons scattered from polycrystalline uranium dioxide at 783°K. (Average of three scattering angles).

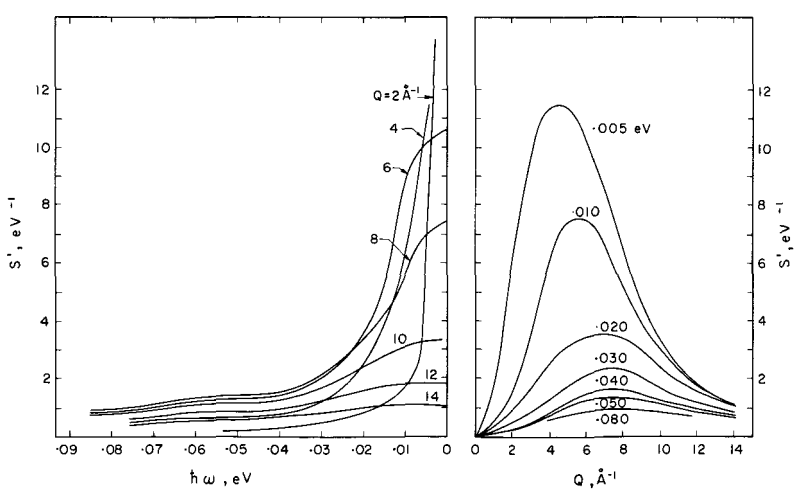

Fig. 12 - The scattering function $S'(Q,\epsilon)$ for protons in light water at 298°K. σ_b = 81.5 barn.

and the energy to wavelength conversion. The quasi-elastic component of the scattering [32, 35] from water which has a form factor of approximately $\exp(-0.45\ Q^2)$ is not included in Fig. 12.

The distribution of neutrons scattered from UO_2 at 783°K is shown in Fig. 11. The peaks in the distribution at 1.12 Å and 1.43 Å probably indicate structure in the frequency distribution of the normal modes of vibration at $\epsilon = 11$ meV, but the frequency distribution can only be deduced with the aid of supplementary information on the amplitudes of the vibrations. The large peak at 1.26 Å is the unresolved Debye-Scherrer elastic scattering from several planes of the polycrystalline specimen.

7. SUMMARY AND ACKNOWLEDGMENTS

This paper presents a brief outline of inelastic neutron scattering measurements carried out at the NRU reactor at Chalk River. It does not purport to be a comprehensive survey or a historical record. We are indebted to the many colleagues who have been associated with the experiments described herein. We thank B.A. Dasannacharya and K.R. Rao for communicating unpublished results (Fig. 8).

[1] VAN HOVE, L., Phys. Rev. **95** (1954) 249-262.
[2] BROCKHOUSE, B.N., in Proc. Symp. Inelastic Scattering of Neutrons in Solids and Liquids, Vienna (1961) 113-157.
[3] McALPIN, W., publication AECL-1695 Atomic Energy of Canada Limited, Chalk River (1963); also Nuclear Instr. and Methods **25** (1964) 205-
[4] WOODS, A.D.B. *et alii,* in Proc. Symp. Inelastic Scattering of Neutrons in Solids and Liquids, Vienna (1961) 487-500.
[5] EGELSTAFF, P.A. *et alii,* in Proc. Symp. Inelastic Scattering of Neutrons in Solids and Liquids, Vienna (1961) 165-177.
[6] BORN, M. and HUANG, K., *Dynamical theory of crystal lattices,* London (1954).
[7] WOODS, A.D.B. *et alii,* Phys. Rev. **131** (1963) 1025-1029; also WOODS, A.D.B. *et alii,* Phys. Rev. **119** (1960) 980-999.
[8] NAKAGAWA, Y. and WOODS, A.D.B., Phys. Rev. Letters **11** (1963) 271-274; also *Lattice dynamics of niobium* submitted to J. Phys. and Chem. Solids.
[9] CHEN, S.H. and WOODS, A.D.B., Bull. Amer. Phys. Soc. **9** (1964) 83.
[10] WOODS, A.D.B., Bull. Amer. Phys. Soc. **9** (1964) 83.
[11] CHEN, S.H. and BROCKHOUSE, B.N., *Lattice vibrations of tungsten,* submitted to Solid State Communications.
[12] BIRGENEAU, R.J. *et alii, Normal vibrations of nickel,* submitted to Bull. Amer. Phys. Soc.
[13] DOLLING, G. and BROCKHOUSE, B.N., Phys. Rev. **128** (1962) 1120-1123.
[14] BROCKHOUSE, B.N., Phys. Rev. Letters **2** (1959) 256-258.
[15] DOLLING, G., in Proc. Symp. Inelastic Scattering of Neutrons in Solids and Liquids, **2** - Vienna (1963) 37-48.
[16] BROCKHOUSE, B.N. *et alii,* Proc. Symp. Inelastic Scattering of Neutrons in Solids and Liquids, Vienna (1961) 531-548.
[17] BROCKHOUSE, B.N. *et alii,* Phys. Rev. **128** (1962) 1099-1111.
[18] WOODS, A.D.B. *et alii,* Bull. Amer. Phys. Soc. **6** (1961) 261.
[19] WOODS, A.D.B. *et alii,* Phys. Rev. **128** (1962) 1112-1120.
[20] GILAT, G. and DOLLING, G., Bull. Amer. Phys. Soc. **9** (1964) 82-83; also *On the temperature dependence of phonons in β-brass* submitted to Solid State Communications.

[21] BROCKHOUSE, B.N. and DASANNACHARYA, B.A., Solid State Communications **1** (1963) 205-209.
[22] WAUGH, J.L.T. and DOLLING, G., Phys. Rev. **132** (1963) 2410-2412; also *Normal vibrations in gallium arsenide* submitted to J. Phys. and Chem. Solids.
[23] COWLEY, R.A., Phys. Rev. Letters **9** (1962) 159-161.
[24] COCHRAN, W., Advances in Phys. **9** (1960) 387-423; and **10** (1961) 401-420.
[25] LYDDANE, R.H. *et alii*, Phys. Rev. **59** (1941) 673-676.
[26] LANDAU, L.D., J. Phys. Acad. Sci. U.S.S.R. **5** (1941) 71-90.
[27] COHEN, M. and FEYNMAN, R.P., Phys. Rev. **107** (1957) 13-24.
[28] HENSHAW, D.G. and WOODS, A.D.B., Phys. Rev. **121** (1961) 1266-1274; and in Proc. VII Intl. Conf. Low Temperature Physics (GRAHAM, G.M. and HALLETT, A.C.H., eds.) Toronto (1961) 539-544.
[29] WOODS, A.D.B., unpublished.
[30] ПИТАЕВСКИЙ, Л.П., ЖЭТФ, **36** (1959) 1168-1178; PITAEVSKII, L.P., Soviet Phys. JETP **9** (1959) 830-837.
[31] BROCKHOUSE, B.N. and POPE, N.K., Phys. Rev. Letters **3** (1959) 259-262.
[32] SAKAMOTO, M. *et alii*, J. Phys. Soc. Japan **17** Suppl. B-II (1962) 370-373.
[33] BROCKHOUSE, B.N. *et alii*, in Proc. Symp. Inelastic Scattering of Neutrons in Solids and Liquids, **1** Vienna (1963) 189-202.
[34] DASANNACHARYA, B.A. and RAO, K.R., unpublished; see also reference [33].
[35] BROCKHOUSE, B.N., Il Nuovo Cim. **9** Suppl. (1958) 45-71.
[36] SINCLAIR, R.N. and BROCKHOUSE, B.N., Phys. Rev. **120** (1960) 1638-1640.
[37] WATANABE, H. and BROCKHOUSE, B.N., Phys. Letters **1** (1962) 189-190.
[38] BROCKHOUSE, B.N. and WATANABE, H., in Proc. Symp. Inelastic Scattering of Neutrons in Solids and Liquids **2** Vienna (1963) 297-308.
[39] KAPLAN, T.A., unpublished; see reference [38].
[40] GLASSER, L.M. and MILFORD, F.J., Phys. Rev. **130** (1963) 1783-1789.
[41] BROCKHOUSE, B.N. *et alii*, J. Phys. Soc. Japan **17** Suppl. B-II (1962) 63-66.
[42] HAYWOOD, B.C. and THORSON, I.M., in Proc. Brookhaven Conf. Neutron Thermalization, publication BNL-719 **1** Brookhaven National Laboratory, Upton, New York (1962) 26-53.
[43] EGELSTAFF, P.A. *et alii*, in Proc. Symp. Inelastic Scattering of Neutrons in Solids and Liquids, **1** Vienna (1963) 343-357.
[44] EGELSTAFF, P.A. and COCKING, S.J., in Proc. Symp. Inelastic Scattering of Neutrons in Solids and Liquids, Vienna (1961) 569-578.
[45] HAYWOOD, B.C. and THORSON, I.M., in Proc. Symp. Inelastic Scattering of Neutrons in Solids and Liquids **2** Vienna (1963) 111-123.
[46] SINCLAIR, R.N., in Proc. Symp. Inelastic Scattering of Neutrons in Solids and Liquids **2** Vienna (1963) 199-211.
[47] HARRIS, D.H.C. and THORSON, I.M., unpublished.